PROCEEDINGS OF SCIENCE

A study of the radiative transition $\pi\pi \to \pi\gamma^*$ with lattice QCD

Luka Leskovec[*a], **Constantia Alexandrou**[b,c], **Giannis Koutsou**[c], **Stefan Meinel**[a,d], **John W. Negele**[e], **Srijit Paul**[c,f], **Marcus Petschlies**[g], **Andrew Pochinsky**[e], **Gumaro Rendon**[a], **Sergey Syritsyn**[d,h]

[a] *Department of Physics, University of Arizona, Tucson, AZ 85721, USA*
[b] *Department of Physics, University of Cyprus, CY 1678 Nicosia, Cyprus*
[c] *Computation-based Science and Technology Research Center, The Cyprus Institute, CY 2121 Nicosia, Cyprus*
[d] *RIKEN BNL Research Center, Brookhaven National Laboratory, Upton, NY 11973, USA*
[e] *Center for Theoretical Physics, Massachusetts Institute of Technology, Cambridge, MA 02139, USA*
[f] *Department of Mathematics and Natural Sciences, University of Wuppertal, D-42119 Wuppertal, Germany*
[g] *Helmholtz-Institut für Strahlen- und Kernphysik, University of Bonn, D-53115 Bonn, Germany*
[h] *Department of Physics and Astronomy, Stony Brook University, Stony Brook, NY 11794, USA*
E-mail: leskovec@email.arizona.edu

Lattice QCD calculations of radiative transitions between hadrons have in the past been limited to processes of hadrons stable under the strong interaction. Recently developed methods for $1 \to 2$ transition matrix elements in a finite volume now enable the determination of radiative decay rates of strongly unstable particles. Our lattice QCD study focuses on the process $\pi\pi \to \pi\gamma^*$, where the ρ meson is present as an enhancement in the cross-section. We use $2+1$ flavors of clover fermions at a pion mass of approximately 320 MeV and a lattice size of approximately 3.6 fm. The required 2-point and 3-point correlation functions are constructed from a set of forward, sequential and stochastic light quark propagators. In addition to determining the ρ meson resonance parameters via the Lüscher method, the scattering phase shift is used in conjunction with the $1 \to 2$ transition matrix element formalism of Briceño, Hansen and Walker-Loud [1] to compute the $\pi\pi \to \pi\gamma^*$ amplitude at several values of the momentum transfer and $\pi\pi$ invariant mass.

34th annual International Symposium on Lattice Field Theory
24-30 July 2016
University of Southampton, UK

*Speaker.

© Copyright owned by the author(s) under the terms of the Creative Commons Attribution-NonCommercial-NoDerivatives 4.0 International License (CC BY-NC-ND 4.0).

arXiv:1611.00282v1 [hep-lat] 1 Nov 2016

1. Introduction

Lattice QCD studies in the past have focused on calculations of hadronic masses within the single-hadron approach, resonance masses and their corresponding strong decay widths via the Lüscher method [2], as well as form factors and matrix elements involving transitions between hadrons stable under the strong interaction. There were also some exploratory calculations of matrix elements involving unstable hadrons, where the effects of the strong decay were neglected [3, 4], leading to uncontrolled finite volume effects.

The effect of the multi-hadron state for the $K \to \pi\pi$ decay was first described by Lellouch and Lüscher [5] and was extended to all elastic states below the inelastic threshold [6]. The Lellouch-Lüscher factor, which encodes the finite volume effects that affect the transition matrix elements, has been generalized to describe also hadrons in a moving frame [7]. The inclusion of multiple decay channel modes of the unstable hadron have been addressed in [8] and a specific setup to calculate the $\Delta \to N\gamma$ decay was proposed in [9]. A recent paper by Briceño, Hansen and Walker-Loud [1] was the first to derive the effects in quantum field theory as well as put forward a full general setup for $1 \to 2$ transition matrix elements involving an arbitrary number of coupled two-hadron channels. The first study employing the formalism of Briceño, Hansen and Walker-Loud (BHWL) was performed by the Hadron Spectrum collaboration only recently [10, 11], for the $\pi\pi(\to \rho) \to \pi\gamma$ transition amplitude. In our work we study the same channel, but use different methods to construct the correlation functions.

2. On the Briceño-Hansen-Walker-Loud formalism

The finite volume effects of the transition matrix element we consider in this work are described by

$$\frac{|F_{IV}(\nu; J_\mu^{QED}; q^2, s_{\pi\pi})|^2}{|\langle n, \Lambda, \nu, \vec{p}_{\pi\pi}|J_\mu^{QED}|\pi, \vec{p}_\pi\rangle|^2} = \frac{32\pi E_\pi \sqrt{s_{\pi\pi}}}{k}\Big[\frac{\partial\delta_1(\sqrt{s_{\pi\pi}})}{\partial E_{\pi\pi}} + \frac{\partial\phi_1^{\vec{p}_{\pi\pi}}(k)}{\partial E_{\pi\pi}}\Big] \tag{2.1}$$

where $\phi_1^{\vec{p}_{\pi\pi}}(k)$ comes from the quantization condition of the Lüscher method, $\cot\delta_1 + \cot\phi_1^{\vec{p}_{\pi\pi}}(k) = 0$, k is related to $\sqrt{s_{\pi\pi}}$ via $\sqrt{s_{\pi\pi}} = 2\sqrt{m_\pi^2 + k^2}$, δ_1 is the phase shift that describes the $\pi\pi$ resonant scattering, $\langle n, \Lambda, \nu, \vec{p}_{\pi\pi}|J_\mu^{QED}|\pi, \vec{p}_\pi\rangle$ is the finite volume matrix element and F_{IV} is the infinite volume matrix element, which can be further reduced by taking into account the Lorentz symmetry. $E_{\pi\pi}$ is the energy of the given state n in the irrep Λ as determined by the spectrum study.

The factor on the right-hand-side is referred to as the Lellouch-Lüscher factor [5] and represents the mapping from the finite volume matrix element to the infinite volume transition amplitude. The basic idea of the BHWL formalism is to calculate the Lellouch-Lüscher factor using prior knowledge and then perform the mapping from the finite volume to the infinite volume. This is done not only for the ground state, but for all relevant states in the lattice irrep in which the unstable hadron, in our case the ρ, is present.

Thus, an essential part of the BHWL formalism is the spectroscopy study, where the phase shift in a given channel (in our case elastic $\pi\pi$ scattering) is calculated with the Lüscher method and its generalizations [2]. This provides us with two quantities - the phase shift needed to determine the mapping, and the specific linear combinations of interpolating operators that create a well

defined specific state. These combinations yield the optimized correlators [12], and give us access to the matrix elements at several different values of the $\pi\pi$ invariant mass. A simple outline of the procedure we employ to determine the infinite volume amplitude looks like:

1) perform a lattice calculation of $\pi\pi$ p-wave resonant scattering in the multi-hadron approach and determine the phase shift with the Lüscher method

2) determine the parameters of the Breit-Wigner phase shift form and calculate the derivative of the phase shift with respect to the two-particle energy for the given Breit-Wigner parametrization

3) calculate the $\pi\pi \to \pi\gamma$ three point functions involving both $\bar{q}\Gamma_i q$ and $\pi\pi$ interpolating operators and utilize the information from 1) to project them to definite states

4) use the derivative of the phase shift from 2) combined with the function $\frac{\partial \phi_1^{\vec{p}\pi\pi}(k)}{\partial E_{\pi\pi}}$ to determine the mapping from the finite volume matrix elements to the infinite volume amplitude.

3. Construction of the correlation functions

To calculate the 2-point and 3-point correlation functions we adapted a method using a combination of forward, sequential, and stochastic propagators. The forward quark propagator S_f from the initial point $(\vec{x}_i, t_i)$ to the final point $(\vec{x}_f, t_f)$ is the inverse of the Dirac operator D:

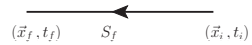

$$S_f(\vec{x}_f, t_f; \vec{x}_i, t_i)^{ab}_{\alpha\beta} = D^{-1}(\vec{x}, t_f; \vec{x}_i, t_i)^{ab}_{\alpha\beta}\,, \tag{3.1}$$

where α, β are spin indices and a, b are color indices. The sequential propagator describes a quark flow through a vertex of a given flavor and Lorentz structure. It is obtained by using the product of a forward propagator and the gamma matrix in the vertex as a the source for the solver. It requires 12 inversions (one for each spin and color index) for each distinct sequential source time t_{seq}, momentum $\vec{p}$ and and Γ matrix:

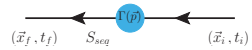

$$\begin{aligned} &S_{seq}(\vec{x}_f, t_f; \vec{x}_i, t_i; t_{seq}, \vec{p}, \Gamma) \\ &\quad = \sum_{\vec{x}_{seq}} D^{-1}(\vec{x}_f, t_f; \vec{x}_{seq}, t_{seq})\, \Gamma\, e^{i\vec{p}\vec{x}_{seq}}\, S_f(\vec{x}_{seq}, t_{seq}; \vec{x}_i, t_i)\,. \end{aligned} \tag{3.2}$$

The stochastic timeslice-to-all propagator is defined as by the inversion of the Dirac matrix on a stochastic timeslice momentum source:

$$\begin{aligned} \phi(t_i, \vec{p}) &= D^{-1}\, \xi(t_i, \vec{p}) \\ \xi(t_i, \vec{p}_i)_{t,\vec{x},\beta,b} &= \sum_{\vec{y}} \delta_{t,t_i}\, e^{i\vec{p}_i\vec{y}}\, \xi(t_i)_{\vec{y},\beta,b}\,. \end{aligned} \tag{3.3}$$

This technique provides an efficient way to evaluate the partially disconnected diagrams involved in typical multi-hadron studies with reasonable cost. In addition to time-dilution of the stochastic momentum source, we also apply spin-dilution to make use of the efficient one-end-trick in our contractions:

$$\xi(t_i, \vec{p}_i, \alpha)_{t,\vec{x},\beta,b} = \sum_{\vec{y}} \delta_{t,t_i}\, \delta_{\alpha,\beta}\, e^{i\vec{p}_i\vec{y}}\, \xi(t_i)_{\vec{y},b}\,. \tag{3.4}$$

To enhance the overlap to the low lying states contributing to a correlator we apply source and sink smearing to the propagator types listed above by replacing $S_X \to W S_X W^\dagger$, where W denotes the Wuppertal-smearing operator [13] and $X \in \{f, seq, st\}$.

To determine the $\pi\pi$ p-wave phase shift we calculate the 2-point correlation functions in the multi-hadron approach, within which we build a correlation matrix $C_{ij}(t) = \langle O_i(t) O_j^\dagger(0) \rangle$ from two types of interpolating operators $O^{\bar{q}q}$ and $O^{\pi\pi}$:

$$\begin{aligned} O_\nu^{\bar{q}q} &\sim \bar{q}\Gamma_\nu q(\vec{p}_{\pi\pi}), \\ O_\nu^{\pi\pi} &\sim \pi^+(\vec{p}_1)\pi^-(\vec{p}_2), \end{aligned} \tag{3.5}$$

where $\vec{p}_{\pi\pi} = \vec{p}_1 + \vec{p}_2$ and $\Gamma_\nu = \{\gamma_\nu, \gamma_4\gamma_\nu\}$. We project these correlation functions to definite $\pi\pi$ momenta, where $\vec{p}_{\pi\pi} = \frac{2\pi}{L}(0,0,0)$, $\frac{2\pi}{L}(0,0,1)$, $\frac{2\pi}{L}(0,1,1)$ and their permutations. We combine the interpolators in such a manner that each is in a well defined irreducible representation, which are constructed by the projection operator defined in Eq. (13) of [14].

Schematically, the Wick diagrams involved in constructing the correlation matrix are presented in Figure 1 and are built using the propagators defined above.

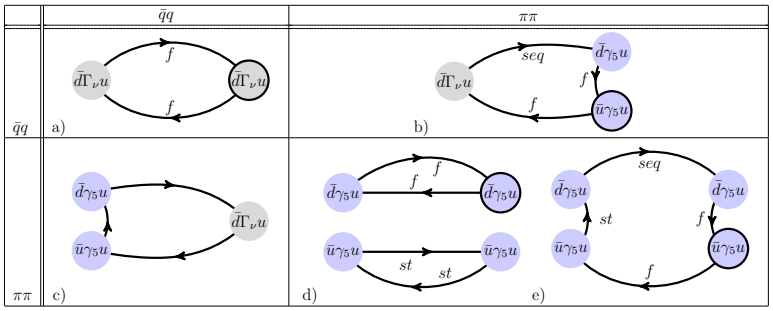

Figure 1: The correlation matrix C_{ij} for the 2-point functions, which involves 4 types of diagrams that are built from the propagators defined in Section 3.

The spectrum in each of the momentum frames and irreps is obtained by solving the generalized eigenvalue problem (for details on GEVP see [15] and [16]) $C(t)u_n(t) = \lambda_n(t,t_0)C(t_0)u_n(t)$. We use $t_0 = 2$ and checked that for t_0 up to 6 the spectrum is consistent with our choice.

The $(I)J^{PC} = (1)1^{--}$ elastic $\pi\pi$ scattering phase shift is obtained using the Lüscher method [2] as well as its generalizations [17, 18]. The relevant equations for the mapping from the finite volume to the infinite volume are listed in [19], and a comparison of previous studies can be found in [20].

To determine the 3-point correlation functions C_3 that project to a definite state in the irreducible representation, we calculate the 3-point functions C_3^i:

$$C_3^i(t_J,t_i,t_f) = \sum_{n\in\Lambda,\vec{p}_{\pi\pi}} \langle 0|O_i|n,\Lambda,\nu\rangle\langle n,\Lambda,\nu,|J^\mu_{QED}|\pi,\vec{p}_\pi\rangle\langle\pi|O_\pi|0\rangle \frac{e^{-E_n(t_f-t_J)}e^{-E_\pi(t_J-t_i)}}{2E_\pi E_n}, \tag{3.6}$$

where t_J is the current insertion timeslice, t_i is the pion creation timeslice and t_f is the $\pi\pi$ channel annihilation timeslice. J_μ^{QED} is the QED current, $J_\mu^{QED} = Z_V(\frac{2}{3}\bar{u}\gamma_\mu u - \frac{1}{3}\bar{d}\gamma_\mu d)$ and $Z_V = 0.79700(24)$. The index i runs over the interpolators used in the 2-point function part and includes

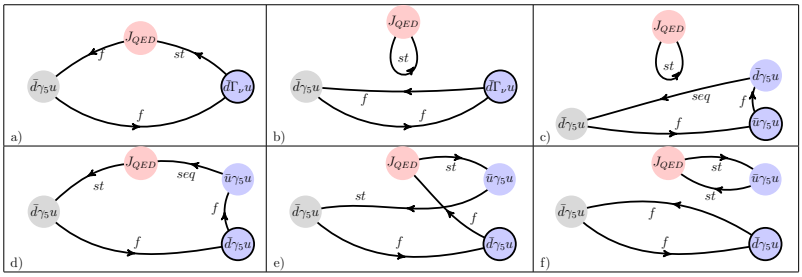

Figure 2: Wick diagrams for the 3-point correlation functions. We have not yet included the disconnected diagrams in b) and c) to the correlation function.

both the $\pi\pi$ and $\bar{q}q$ interpolators to describe the $\rho/\pi\pi$ state. All the relevant 3-point functions are shown in Fig. 2, however we have not yet included the disconnected terms in Fig. 2b) and c).

The projection to the definite state is done by using the idea of the optimized correlator [12, 21, 22] to construct combination of the C_3^i that will have the best possible overlap to a given state, $C_3(n,t_J,t_i,t_f) = u_n^i C_3^i(t_J,t_i,t_f)$. To determine the matrix elements $\langle n,\Lambda,\nu,\vec{p}_{\pi\pi}|J_\mu^{QED}|\pi,\vec{p}_\pi\rangle$, where n marks the state in the irrep Λ with polarization ν and momentum $\vec{p}_{\pi\pi}$, from the 3-point functions, we use a ratio similar to those defined in [23]:

$$R(n,t_J,t_i,t_f) = \frac{C_3(n,t_J,t_i,t_f)C_3^*(n,t_f+t_i-t_J,t_i,t_f)}{C_2^{(n)}(t_f,t_i)C_2^{(\pi)}(t_f,t_i)} \to |\langle n,\Lambda,\nu,\vec{p}_{\pi\pi}|J_{QED}^\mu|\pi,\vec{p}_\pi\rangle|^2. \tag{3.7}$$

We determine the amplitude $|F_{IV}(\nu;J_\mu^{QED};q^2,s_{\pi\pi})|$ for the $\pi\pi \to \pi\gamma$ transition by mapping the finite volume matrix elements to the infinite volume matrix elements using Eq. (2.1) and then performing the Lorentz invariant decomposition:

$$F_{IV}(\nu;J_\mu^{QED};q^2,s_{\pi\pi}) = f_{\pi\pi,\pi}(q^2,s_{\pi\pi})\varepsilon_{\mu\nu\alpha\beta}(p_{\pi\pi})_\alpha(p_\pi)_\beta, \tag{3.8}$$

where $q = p_\pi - p_{\pi\pi}$ and $f_{\pi\pi,\pi}$ is the Lorentz invariant amplitude.

4. Preliminary results and conclusions

Our results are obtained on a $32^3 \times 96$ lattice gauge ensemble with $N_f = 2+1$ dynamical clover-Wilson fermions, which is described in detail in ref. [24]. The light quark mass corresponds to a pion mass of 317(2) MeV with a lattice spacing of $a = 0.11403(77)$ fm. The presented results are obtained from a subset of $N_{conf} = 367$ configurations available on this lattice.

The $(I)J^{PC} = (1)1^{--}$ elastic $\pi\pi$ scattering phase shift is shown in Fig. 3. By fitting a Breit-Wigner form to the phase shift we obtain the following parameters for the ρ resonance, which is present in this channel:

$$\tan\delta_1(\sqrt{s_{\pi\pi}}) = \frac{\sqrt{s_{\pi\pi}}\,\Gamma(\sqrt{s_{\pi\pi}})}{m_\rho^2 - s_{\pi\pi}}, \qquad \Gamma(\sqrt{s_{\pi\pi}}) = \frac{g_{\rho\pi\pi}^2}{6\pi}\frac{k^3}{s_{\pi\pi}} \tag{4.1}$$

$$m_\rho = 798.2(5.3)\text{ MeV} \qquad g_{\rho\pi\pi} = 6.46(53) \tag{4.2}$$

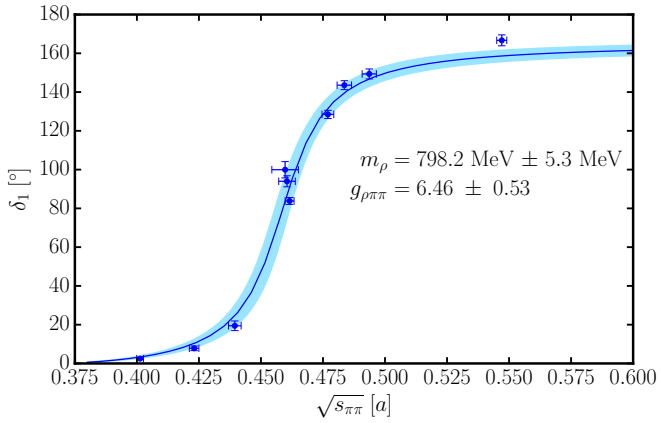

Figure 3: The $\pi\pi$ scattering phase shift as calculated on our gauge ensemble with $m_\pi = 317(2)$ MeV.

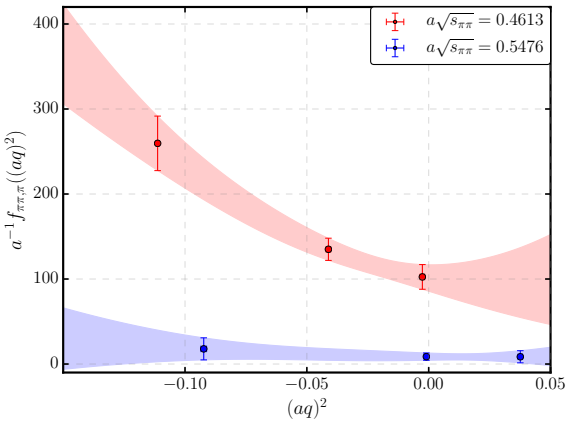

Figure 4: The $\pi\pi \to \pi\gamma$ infinite volume amplitude as determined in the BHWL formalism using $t_f - t_i = 10$. It exhibits an enhancement for $\sqrt{s_{\pi\pi}}$ in the vicinity of the ρ resonance.

The $\pi\pi \to \pi\gamma$ infinite volume amplitude is shown in Fig. 4. It exhibits the basic expected features, including an amplification near $\sqrt{s_{\pi\pi}} \approx m_\rho$. Our results are comparable with the results in a previous study by the Hadron Spectrum collaboration [10, 11]. The adapted method for constructing correlation functions is computationally efficient on large volumes and produces good quality of data.

5. Acknowledgement

We are grateful to Kostas Orginos for providing the gauge ensemble generated with resources provided by XSEDE, which is supported by National Science Foundation grant number ACI-1053575. Our calculations were performed at NERSC, supported by the U.S. DOE under Contract No. DE-AC02-05CH11231. SM and GR are supported by NSF grant PHY-1520996. SM and SS also thank the RIKEN BNL Research Center for support. JN was supported in part by the DOE

Office of Nuclear Physics under grant #DE-FG02-94ER40818. AP was supported in part by the U.S. Department of Energy Office of Nuclear Physics under grant #DE-FC02-06ER41444. SP is supported by the Horizon 2020 of the European Commission research and innovation programme under the Marie Sklodowska-Curie grant agreement No. 642069.

References

[1] R. A. Briceño, M. T. Hansen, and A. Walker-Loud, Phys. Rev. **D91**, 034501 (2015), 1406.5965.

[2] M. Luscher, Nucl. Phys. **B354**, 531 (1991).

[3] M. Crisafulli and V. Lubicz, Phys. Lett. **B278**, 323 (1992).

[4] R. R. Horgan, Z. Liu, S. Meinel, and M. Wingate, Phys. Rev. Lett. **112**, 212003 (2014), 1310.3887.

[5] L. Lellouch and M. Luscher, Commun. Math. Phys. **219**, 31 (2001), hep-lat/0003023.

[6] C. J. D. Lin, G. Martinelli, C. T. Sachrajda, and M. Testa, Nucl. Phys. **B619**, 467 (2001), hep-lat/0104006.

[7] N. H. Christ, C. Kim, and T. Yamazaki, Phys. Rev. **D72**, 114506 (2005), hep-lat/0507009.

[8] M. T. Hansen and S. R. Sharpe, Phys. Rev. **D86**, 016007 (2012), 1204.0826.

[9] A. Agadjanov, V. Bernard, U. G. Meißner, and A. Rusetsky, Nucl. Phys. **B886**, 1199 (2014), 1405.3476.

[10] R. A. Briceno *et al.*, Phys. Rev. Lett. **115**, 242001 (2015), 1507.06622.

[11] R. A. Briceño *et al.*, Phys. Rev. **D93**, 114508 (2016), 1604.03530.

[12] J. J. Dudek, R. Edwards, and C. E. Thomas, Phys. Rev. **D79**, 094504 (2009), 0902.2241.

[13] S. Gusken *et al.*, Phys. Lett. **B227**, 266 (1989).

[14] X. Feng, K. Jansen, and D. B. Renner, Phys. Rev. **D83**, 094505 (2011), 1011.5288.

[15] B. Blossier, M. Della Morte, G. von Hippel, T. Mendes, and R. Sommer, JHEP **04**, 094 (2009), 0902.1265.

[16] K. Orginos and D. Richards, J. Phys. **G42**, 034011 (2015).

[17] K. Rummukainen and S. A. Gottlieb, Nucl. Phys. **B450**, 397 (1995), hep-lat/9503028.

[18] R. A. Briceno, Phys. Rev. **D89**, 074507 (2014), 1401.3312.

[19] Hadron Spectrum, J. J. Dudek, R. G. Edwards, and C. E. Thomas, Phys. Rev. **D87**, 034505 (2013), 1212.0830, [Erratum: Phys. Rev.D90,no.9,099902(2014)].

[20] RQCD, G. S. Bali *et al.*, Phys. Rev. **D93**, 054509 (2016), 1512.08678.

[21] D. Bečirević, M. Kruse, and F. Sanfilippo, JHEP **05**, 014 (2015), 1411.6426.

[22] C. J. Shultz, J. J. Dudek, and R. G. Edwards, Phys. Rev. **D91**, 114501 (2015), 1501.07457.

[23] W. Detmold, C. Lehner, and S. Meinel, Phys. Rev. **D92**, 034503 (2015), 1503.01421.

[24] J. Green *et al.*, Phys. Rev. **D92**, 031501 (2015), 1505.01803.